

SOLIDIFICATION OF A CORNSTARCH AND WATER SUSPENSION

SOLIDIFICACIÓN DE UNA SUSPENSIÓN DE MAICENA Y AGUA

S. R. WAITUKAITIS[†] AND H. M. JAEGER

The James Franck Institute and The Department of Physics, The University of Chicago, USA, swaitukaitis@uchicago.edu[†]

[†] corresponding author

We report on an investigation of the solidification of a cornstarch and water suspension during normal impact on its surface. We find that a finite time after impact, the suspension displays characteristics reminiscent of a solid, including localized stress transmission, the development of a yield stress, and some elastic energy storage. The time dependence of these characteristics depends on the thickness of the cornstarch layer, showing that the solidification is a dynamic process driven by the impacting object. These findings confirm previous speculations that rapidly applied normal stress transforms the normally fluid-like suspension into a temporarily jammed solid and draw a clear distinction between the effects of normal stress and shear stress in dense suspensions.

Se presenta una investigación de la solidificación de una suspensión de maicena y agua durante el impacto normal en su superficie. Se encuentra que, un tiempo finito después del impacto, la suspensión presenta características de un sólido, incluyendo la transmisión local de estrés, el desarrollo de un límite de elasticidad, y el almacenamiento de energía elástica. La evolución temporal de estas características depende del espesor de la capa de maicena, mostrando que la solidificación es un proceso dinámico impulsado por el objeto impactante. Estos resultados confirman anteriores especulaciones sobre la rápida aplicación del estrés normal que transforma la suspensión del estado fluido a un estado atascado temporalmente y establecen una distinción clara entre los efectos de la aplicación del estrés normal y el estrés tangencial en suspensiones densas.

PACS: Shock waves in fluid dynamics, 47.40.Nm; suspensions complex fluids, 47.57.E-; liquid-solid transitions, 64.70.D-

INTRODUCTION

Shear-thickening suspensions, such as a mixture of cornstarch and water, are typically studied in rheometry experiments where shear or tensile stress is measured as a function of the shear rate [1, 2, 3, 4]. The results of these experiments are typically categorized as either reversible or discontinuous. In the former, the change in the suspension's apparent viscosity is small and is generally attributed to the formation of "hydroclusters", small groups of particles interacting through lubrication forces [1, 2, 5, 6]. In the latter, the change in viscosity can appear divergent. This behavior is often associated with forcing the particulate phase across the jamming threshold [3, 4, 7, 8, 9], similar to the creation of "shear-jammed" states in dry granular systems [10]. While these experiments are relevant to the investigation of steady-state shear phenomena, they cannot be expected to apply to large-scale, transient disturbances such as the response during rapidly applied normal stress on the suspension surface. Recent experiments [14, 15] with driven, immersed spheres have shown that applied normal stress can lead to jammed regions of suspension transmitting stress to system boundaries. Even so, these measurements have not given the details of how such jammed regions form. We study this solidification process by investigating the stress transmission through a suspension of cornstarch and water during surface impact. Our results show that the growth of the jammed region is directly linked to the dynamics of the disturbance.

RESULTS AND DISCUSSION

The experimental apparatus is shown in Fig. 1. An aluminum rod ($D = 1.86 \text{ cm}$, $M = 0.368 \text{ kg}$) is allowed to fall-freely or is shot via slingshot into a large tub ($30 \times 30 \times 30 \text{ cm}$) of cornstarch and water suspension. The precise time of impact is determined with the aid of an accelerometer embedded in the rod as well as a high-speed camera, which gives independent access to the instantaneous rod velocity and position. An immersed force sensor simultaneously records the stress transmitted to the container bottom directly below the rod.

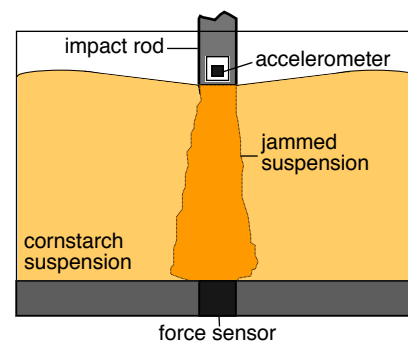


Figure 1: Experimental setup. The impact rod (grey) hits the cornstarch surface, creating a jammed region of suspension (dark orange) which transmits stress to the force sensor at the container bottom.

Fig. 2 shows a typical profile for the force on the rod F_{rod} and the force on the sensor at the container bottom F_b as a function of the time after impact with a fill height $H = 10.5 \text{ cm}$ (impact velocity $v_0 = 2.0 \text{ m/s}$, packing fraction $\phi = 0.49$ and suspending fluid viscosity $\eta = 1.0 \text{ cP}$). Even for modest impact velocities, this produces an incredibly large force on the rod. In this case, the maximum pressure on the rod face is about 500 kPa and the maximum deceleration $\sim 35 \text{ g}$. The peak force on the rod does not necessarily show temporal correspondence with the peak force on the container bottom, indicating that the force on the rod is not solely a consequence of stress transmission to the container bottom (as is the case for smaller H). For the value of H in Fig. 2, a slow initial buildup of the force measured on the container bottom F_b is followed by an abrupt jump to its maximum value of $\sim 7 \text{ N}$ at $t \approx 7.5 \text{ ms}$. After this, F_b and F_{rod} slowly die away. This is a consequence of both the slowing of the rod as the transmitted force decelerates it and also the concomitant “melting” of the suspension, as is described in the experiments [14] of von Kann *et al.* Given the area of the sensor is 1.13 cm^2 and assuming the pressure on the bottom is roughly constant, we estimate that the total force on the rod is recovered over an area $\sim 10 \text{ cm}^2$. This is much smaller than the full area of the container bottom (900 cm^2), and if we imagine the stress propagates through the suspension in a cone this corresponds to an angle of about 10° (we remark that this likely underestimates the cone angle given that the pressure is presumably not constant and highest directly below the rod).

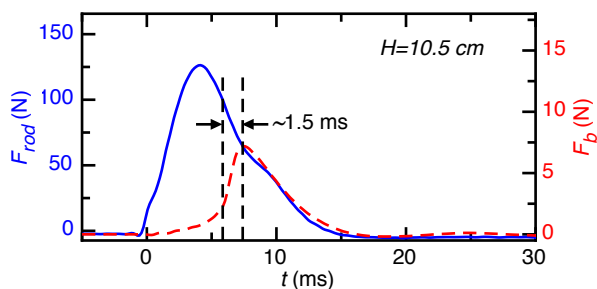


Figure 2: Force on rod F_{rod} (blue curve, left axis) and container bottom F_b (red dashed curve, right axis) vs. time after impact t .

The localization evident from Fig. 2 is the first signature jammed region of suspension transmitting the force on the rod to the container bottom in the manner of a solid. Once this solidified region has formed and reaches bottom, other solid-like behaviors are present. For example, in sufficiently shallow containers and sufficiently high impact speeds, the impacting rod can maintain large amounts of momentum once the growing solid has reached bottom. Rather than yielding and flowing along the bottom, however, the solid compresses, stores energy, and causes the rod to bounce off of the suspension surface. Although it is in principle possible that this energy storage comes from dilation causing grains to poke out from the liquid-air interface [3, 7, 8], we can rule out this possibility by observing that the presence a thin water layer on the suspension surface ($\sim 0.5 - 1.0 \text{ cm}$, which prevents particles from interacting with the air-water interface) does not eliminate the bounce. This leads us to conclude that the energy is in fact stored and released by compression of the grains, as

is encountered for the elasto-hydrodynamic collision between fluid-coated steel spheres in “Stoke’s Cradle” experiments [11, 12, 13]. In addition to transmitting stress locally on the container bottom, the jammed region also has a yield stress and can store elastic energy.

We can use shape of the F_b vs. t curves to probe the dynamic details of the solidification process. In particular, the time of the peak can be thought of as the time required for the leading edge of the growing solid to reach the lower boundary. In Fig. 2, for example, knowing that the peak occurs at $t \approx 7.5 \text{ ms}$ and $H = 10.5 \text{ cm}$ allows us to determine that, on average, the suspension solidifies at a rate of $\sim 15 \text{ m/s}$ (for $v_0 = 2.0 \text{ m/s}$). From the sharp upturn to the peak in Fig. 2 (from about $5 - 7 \text{ ms}$), we can make a rough estimate of the width of the leading edge of the solidification region as $\delta \approx v_0 \Delta t \approx 4 \text{ mm}$. Given that once the solid reaches bottom it must compress a little to develop the peak in F_b , this is likely an overestimate of the front width, but even so it indicates that the front is spatially well-defined in comparison to the size of the solidified region once it hits bottom ($\sim 10 \text{ cm}$).

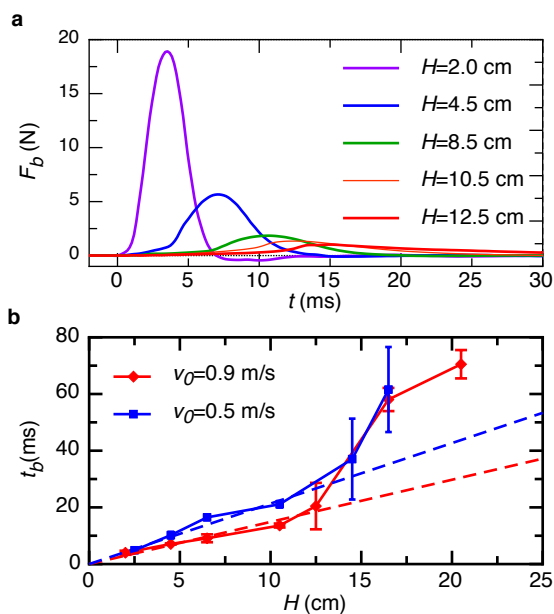


Figure 3: (a) Force on the container bottom (F_b) vs. time for impact at $v_0 = 0.9 \text{ m/s}$ and different fill heights H . (b) Time t_b for the peak in F_b vs. container height H . The error bars show the standard deviations over 3+ individual measurements.

We can gain more insight into this time-dependent solidification by investigating the F_b vs. t curves for different H , as in Fig. 3 (a). As might be expected, the scale of the recovered force decreases monotonically with increasing H and occurs later in time. The weaker force is a result of the decreased speed of the rod when the solid hits bottom as well as the continued spreading of the stress-cone for deeper containers. Plotting the time of the force peak t_b vs. H maps a trajectory of the solid growth, as in Fig. 3 (b). Rather than growing at a constant velocity, the solid develops quickly at first and then slows down. This is reminiscent of the rod trajectory and suggests that the speed of growth is influenced by the speed of the rod (see ref. [16] for example). To test this, we can plot the front

trajectories for different impact speeds, which shows that higher speed impacts produce fronts with faster initial speeds (see the curves for $v_0 = 0.5$ and 0.9 m/s in Fig. 3 (b)). From fitting the portions of these curves before the slow-down we obtain an initial growth rate ~ 10 times faster than the speed of impact.

At first glance, the dependence of the solidification speed on the rod velocity seems similar to shocks in jammed granular systems [17]. A closer look, however, reveals important differences. The speed at which these fronts propagate seems to scale linearly with the impact speed. In the jammed granular system, two types of propagation are encountered, neither of which scale linearly. In the first case, when the impact speed is low, the front speed is constant and is simply set by the degree to which the grains are pre-compressed before impact (this is essentially sound propagation). In the case of high impact speed, the front speed scales like $v^{1/5}$ as a consequence of the impact causing the already compressed grains to compress further still. These sharp differences can be understood simply by realizing that the system here, unlike the granular system, is *not jammed* before impact; the impact causes it to jam. Given that it is initially unjammed, it cannot support sound propagation through the particle matrix, and it is therefore not surprising that the front speed is not constant but instead depends on the impactor velocity.

CONCLUSIONS

While previous experiments have suggested that under applied normal stress solidified regions of suspension can transmit stress to boundaries, our results give insight into the dynamic details of how this solidification occurs. We show that the solidified region is highly localized, extending over a very small area on the opposing boundary from the impact site. We find that the speed at which the suspension solidifies is set by the speed of the disturbance, with faster solidification occurring for more rapidly applied stress, and that the fronts are spatially well-defined. These results highlight distinct differences between steady-state, shear driven situations and phenomena driven by normal stress, showing that the latter is dominated by the inherently transient character of driving the suspension into the jammed state.

ACKNOWLEDGEMENTS

We thank Wendy Zhang, Tom Witten, Vincenzo Vitelli, Carlos

Orellana, Sidney Nagel, Marc Miskin, William Irvine, Qiti Guo, Jake Ellowitz, Justin Burton, and Eric Brown for insightful discussions. This work was supported by the NSF through its MRSEC program (DMR-0820054). S. R. W. acknowledges support from a Millikan fellowship.

-
- [1] N. J. Wagner and J. F. Brady, *Physics Today* **62**, 27 (2009).
 - [2] X. Cheng, J. H. McCoy, J. N. Israelachvili and I. Cohen, *Science* **333**, 1276 (2011).
 - [3] E. Brown, N. A. Forman, C. S. Orellana, H. Zhang, B. W. Maynor, D. E. Betts, J. M. DeSimone and H. M. Jaeger *Nature Materials* **9**, 220 (2010).
 - [4] E. E. Bischoff-White, M. Chellamuthu and J. P. Rothstein, *Rheol. Acta* **49**, 119 (2010).
 - [5] J. F. Brady and G. Bossis, *Annu. Rev. Fluid Mech.* **20**, 111 (1988).
 - [6] B. J. Maranzano and N. J. Wagner, *J. Chem. Phys.* **114**, 10514 (2001).
 - [7] E. Brown, H. Zhang, N. A. Forman, B. W. Maynor, D. E. Betts, J. M. DeSimone and H. M. Jaeger, *Phys. Rev. E* **84**, 031408, (2011).
 - [8] E. Brown and H. M. Jaeger, *M. Phys. Rev. Lett.* **103**, 086001 (2009).
 - [9] M. E. Cates, M. D. Haw and C. B. Holmes, *J. of Phys: Cond. Matt.* **17**, S2517 (2005).
 - [10] D. Bi, J. Zhang, B. Chakraborty and R. P. Behringer, *Nature* **480**, 355 (2011).
 - [11] R. H. Davis and J. -M. Serayssol, *J. Fluid Mech.* **163**, 479 (1986).
 - [12] C. Donahue, C. Hrenya and R. Davis, *Phys. Rev. Lett.* **105**, 034501 (2010).
 - [13] C. Donahue, C. Hrenya, R. Davis, K. Nakagawa, A. Zelinskaya and G. Joseph, *J. Fluid Mech.* **650**, 479504 (2010).
 - [14] S. von Kann, J. H. Snoeijer, D. Lohse and D. van der Meer, *Phys. Rev. E* **84**, 060401 (2011).
 - [15] B. Liu, M. Shelley and J. Zhang, *Phys. Rev. Lett.* **105**, 188301 (2010).
 - [16] S. R. Waitukaitis and H. M. Jaeger, *Nature* **487**, 205 (2012).
 - [17] L. R. Gómez, A. M. Turner, M. van Hecke and V. Vitelli, *Phys. Rev. Lett.* **108**, 058001 (2012).